

Local anisotropy in incompressible magnetohydrodynamic turbulence

L. J. Milano, W. H. Matthaeus, and P. Dmitruk

Bartol Research Institute, University of Delaware, Newark, Delaware 19716

D. C. Montgomery

Department of Physics and Astronomy, Dartmouth College, Hanover, New Hampshire 03755-3528

(Received 13 December 2000; accepted 2 March 2001)

It is a well known fact that in the presence of a dc applied magnetic field, magnetohydrodynamic (MHD) turbulence develops spectral anisotropy from isotropic initial conditions. Typically, the reduced spectrum is steeper in the direction of the magnetic field than it is in any transverse direction. One might expect that a dc field is not essential, and it is the local mean field that is responsible. To address this issue, three-dimensional MHD pseudo-spectral incompressible relaxation simulations are performed, and structure functions computed according to whether the separation is parallel to, or transverse to, the local mean magnetic field. Correlation lengths are longer in the locally averaged magnetic field direction than in any perpendicular direction, even when the global mean magnetic field is zero. Local anisotropy is observed to be stronger in regions of strong magnetic field. A general definition of anisotropy angles and a methodology to study local anisotropy are proposed. © 2001 American Institute of Physics. [DOI: 10.1063/1.1369658]

I. INTRODUCTION

It is very well established that in the presence of a dc (constant both in space and time) applied magnetic field, magnetohydrodynamic (MHD) turbulence develops spectral anisotropy from an isotropic initial condition.^{1,2} The reduced spectrum is steeper in the direction of the dc magnetic field than it is in any transverse direction. The turbulent cascade transfers energy to the perpendicular wavenumbers up to the dissipation scale in the usual way, but no cascade occurs in the parallel direction.²⁻⁷ This theoretical picture is supported by experiments,⁸⁻¹⁰ astrophysical observations^{11,12} and numerical simulations.^{2,5,6,13} Its full implications in MHD turbulence theory are diverse, and have not yet been completely realized.

A simple and intuitive interpretation of spectral anisotropy was given in Ref. 2. In incompressible MHD all nonlinear interactions occur among triads of wavevectors satisfying $\mathbf{k}_1 = \mathbf{k}_2 + \mathbf{k}_3$. In the presence of a dc magnetic field \mathbf{B}_{dc} , a perturbative analysis shows that for resonant triads, one of the members must satisfy $\mathbf{k} \cdot \mathbf{B}_{dc} = 0$, and the other two have an equal and opposite component in the direction parallel to \mathbf{B}_{dc} . Thus, resonant spectral transfer can only increase the perpendicular component of the wavevectors. The relevance of these triad interactions was first put into doubt¹⁴ and later on confirmed^{3,15,16} by different authors.

It is important to note that spectral anisotropy is not confined to the field of weak turbulence, or that of perturbation theory; it is intrinsically related to the structure of the MHD equations. Consider the incompressible MHD equations in the presence of a dc magnetic field \mathbf{B}_{dc} (all magnetic fields in this paper are expressed in velocity units), written in terms of the Elsässer variables $\mathbf{z}^\pm = \mathbf{v} \pm \mathbf{B}$,¹⁷

$$\partial_t \mathbf{z}^\pm = -\mathbf{z}^\mp \cdot \nabla \mathbf{z}^\pm \pm \mathbf{B}_{dc} \cdot \nabla \mathbf{z}^\pm - \frac{1}{\rho} \nabla p + D^\pm, \quad (1)$$

where ρ is the plasma density, p is the total (kinetic plus magnetic) pressure and D^\pm represent the dissipation terms, which are negligible in the inertial range. The first term in the right hand side (RHS) of Eq. (1) represents the nonlinear interactions between the \mathbf{z}^\pm fields, while the second term represents linear (Alfvénic) wave propagation along the dc magnetic field. Rearranging terms in Eq. (1) we obtain

$$\partial_t \mathbf{z}^\pm = -\mathbf{z}^\mp \cdot \nabla_\perp \mathbf{z}^\pm \pm (\mathbf{B}_{dc} \mp \mathbf{z}^\mp) \cdot \nabla_\parallel \mathbf{z}^\pm - \frac{1}{\rho} \nabla p + D^\pm, \quad (2)$$

where we choose \mathbf{B}_{dc} to point in the (0,0,1) direction, $\nabla_\perp = (\partial_x, \partial_y, 0)$ and $\nabla_\parallel = (0, 0, \partial_z)$. Consider the case in which z_0 , the size of the fluctuations, is much smaller than the dc field amplitude. In a turbulent state, the nonlinear term is expected to overcome, or at least to balance the Alfvénic term. It follows from Eq. (2) that these terms are balanced if

$$\frac{|\nabla_\parallel|}{|\nabla_\perp|} \sim \frac{z_0}{B_{dc}}. \quad (3)$$

Thus, parallel variations are much smaller than perpendicular variations, and the ratio is proportional to z_0/B_{dc} .^{5,6} Note that if the nonlinear term overcomes the Alfvénic term, the ratio of typical lengths could be much smaller than what is estimated in Eq. (3). Similar lines of reasoning give place to the reduced MHD (RMHD) equations,¹⁸⁻²¹ which in the last two decades have been widely used in the context of magnetized plasmas, as well as of the ‘‘critically balanced’’ turbulence phenomenology.²²

One might expect that a dc field is not essential, and it is the local mean field that is responsible for inducing dynamic anisotropy. This would be an important consistency result, and gives motivation for the present paper, in which we investigate the occurrence of local anisotropy in three-dimensional MHD. Our main questions are the following: (a) does the local mean magnetic field provide an effective an-

isotropy direction for spatial correlations even in the absence of a dc field? (b) In the presence of a dc field, what is the influence of considering the direction of the local mean (instead of the dc) magnetic field? To answer these questions, we perform three-dimensional (3D) MHD pseudo-spectral incompressible relaxation simulations, and propose a methodology to study local anisotropy, based on the computation of second order structure functions accumulated according to whether the separation is parallel to, or transverse to, the local mean magnetic field.

Spectral anisotropy occurs both in compressible and incompressible MHD turbulence. We note that, in addition to spectral anisotropy, the full (compressible, polytropic) MHD equations verify variance anisotropy (anisotropy in the variance of the Cartesian components of the fluctuating fields) for the strong dc field case (or small plasma β) and low Mach number.²³ That is, the fluctuating components of the velocity field \mathbf{v} and magnetic field \mathbf{b} tend to be perpendicular to the dc magnetic field. Nonetheless, variance anisotropy from an initially isotropic state does not happen in the incompressible cases reported in Refs. 13 and 23 nor in the simulations that we analyze here. We stress the fact that no variance anisotropy is needed to obtain spectral anisotropy, as it is shown for instance in the arguments proceeding from Eq. (3).

The paper is organized as follows. A brief description of the numerical simulations performed is given in Sec. II. The main results of our analysis are reported in Sec. III, and summarized and discussed in Sec. IV. In Appendix A we describe some of the details of the data analysis. Finally, in Appendix B we discuss the relation between the dynamic anisotropy studied in this paper and the well known kinematic anisotropy between longitudinal and lateral structure functions.

II. NUMERICAL SIMULATIONS

We perform a series of 3D MHD incompressible relaxation simulations. We solve the standard MHD incompressible dissipative equations using (under the assumption of periodic boundary conditions) a pseudo-spectral Fourier technique as described in Ref. 13. We label our runs as follows:

- dc run. We let a dc magnetic field $\mathbf{B}_{dc} = B_{dc} \hat{\mathbf{z}}$ act on the plasma, and study the relaxation of the MHD fields $\mathbf{v}(\mathbf{x}, t)$ and $\mathbf{B}(\mathbf{x}, t) = \mathbf{B}_{dc} + \mathbf{b}(\mathbf{x}, t)$.
- ISO run. This is an isotropic run, with no dc field. We let $\mathbf{v}(\mathbf{x}, t)$ and $\mathbf{B}(\mathbf{x}, t) = \mathbf{b}(\mathbf{x}, t)$ relax in time, from an isotropic initial condition with no net mean magnetic field.

Both runs start with isotropic, power-law, random-phase (\mathbf{v} , \mathbf{b}) fields, with unit energy, zero cross helicity and zero magnetic helicity. More explicitly, the initial fields are so that

$$E^v(k) = E^b(k) = \frac{C}{1 + (k/k_{\text{knee}})^{5/3}}, \quad (4)$$

where $k_{\text{knee}} = 4k_0$, k_0 being the smallest wavenumber of the system. $E^v(k)$ and $E^b(k)$ are, respectively, the kinetic and

the magnetic omnidirectional power spectra. We define $L_0 = 2\pi/k_{\text{knee}}$, our ‘‘energy containing scale,’’ as the length unit, u_0 as the velocity and magnetic field unit (recall that the magnetic field is written in velocity units) and $t_0 = L_0/u_0$ as the time unit. The normalization constant C in Eq. (4) is chosen so that $\langle b^2 \rangle = \langle v^2 \rangle = 2\sum_k E^{v,b}(k) = 1$ (at $t=0$). For the dc run, $B_{dc} = 1$ as well. The magnetic Prandtl number is set to 1, the macroscopic Reynolds number is $R = u_0 L_0 / \nu = 200$ and the resolution is 128^3 in all the runs. In all cases the solutions approximately satisfy variance isotropy:

$$\langle v_x^2 \rangle \approx \langle v_y^2 \rangle \approx \langle v_z^2 \rangle, \quad \langle b_x^2 \rangle \approx \langle b_y^2 \rangle \approx \langle b_z^2 \rangle, \quad (5)$$

where the brackets $\langle \rangle$ mean hereafter the spatial average over the whole computational volume. The fluctuating fields \mathbf{v} and \mathbf{b} average to zero at all times: $\langle \mathbf{v} \rangle = 0 = \langle \mathbf{b} \rangle$.

In addition, we perform a hydrodynamic (HD) simulation, that we label ‘‘HYDRO run.’’ Even though our goal in this paper is to study MHD anisotropy, it turns out that a HD run is useful to clarify some aspects of the dynamics, as discussed in Sec. III D. The macroscopic Reynolds number for this run is 200 and resolution 128^3 as in the other two simulations.

III. RESULTS

A. Anisotropy in presence of a dc field

In order to introduce new notation and ideas, while linking them to the familiar case in which a dc external field acts on the fluid, we begin studying the output of the dc run. Since the fluctuations are initially of the same order of magnitude as the dc field, we expect moderate spectral anisotropy. The anisotropy level typically saturates when the dc fields exceed the magnitude of the fluctuations by about a factor 3.^{2,6} Figure 1 shows the reduced spectra at $t=2$. Note that $E_1^{v,b}(k_x) \approx E_1^{v,b}(k_y) > E_1^{v,b}(k_z)$ for wavenumbers in the inertial (and dissipative) range. This is due to the cascade suppression in the parallel direction, induced by the presence of the dc field.²⁻⁷ We recall that the reduced spectra are defined as

$$E_1^{v,b}(k_i) = \sum_{k_j, k_l} E_3^{v,b}(\mathbf{k}) \quad (6)$$

[where $E_3^v(\mathbf{k}) = \frac{1}{2} |\mathbf{v}(\mathbf{k})|^2$ and $E_3^b(\mathbf{k}) = \frac{1}{2} |\mathbf{b}(\mathbf{k})|^2$ are, respectively, the kinetic and magnetic modal energy spectra and $\{i, j, l\}$ denotes any permutation of $\{x, y, z\}$].

Spectral analysis is useful to study global anisotropy, since it involves an expansion of the solutions in Fourier modes. For a local study of anisotropy, a real-space analysis is needed instead. We propose to use second order structure functions of the form

$$S(\mathbf{l}) = \frac{1}{2} \langle |\mathbf{u}(\mathbf{x}) - \mathbf{u}(\mathbf{x} + \mathbf{l})|^2 \rangle, \quad (7)$$

where \mathbf{u} denotes either \mathbf{v} or \mathbf{b} . In Fig. 2, we evaluate Eq. (7) with $\mathbf{l} = l\hat{\mathbf{z}}$ (parallel case) and $\mathbf{l} = l\hat{\mathbf{x}}$ (perpendicular case). Note that both Figs. 1 and 2 reflect the fact that variations in the parallel ($\hat{\mathbf{z}}$) direction are much smoother than the variations in the perpendicular plane. The fluctuating fields remain correlated over longer distances in the parallel direc-

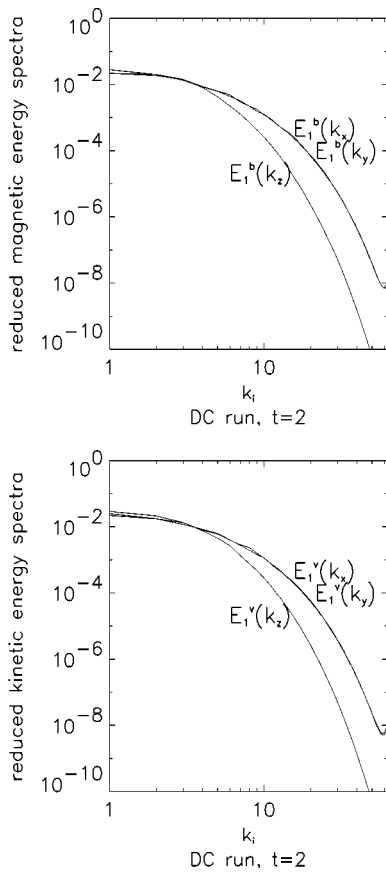


FIG. 1. Reduced energy spectra for the dc run. The parallel direction is given by the dc field, $\mathbf{B}_{dc}=\hat{\mathbf{z}}$. The reduced spectra in the x direction are almost identical to the ones in the y direction, due to isotropy in the perpendicular planes.

tion, than they do in any perpendicular direction. This is indeed the basis for reduced MHD-like models in which turbulence is confined to wavenumbers which are nearly perpendicular to the main, dc magnetic field.

Figure 3 displays structure functions computed following a fairly different approach. We divide the physical space in boxes of size $l_{\text{box}}=\frac{1}{2}L_0$, and define a *local mean magnetic field* \mathbf{B}_0 within each box, as

$$\mathbf{B}_0 \equiv \langle \mathbf{B} \rangle_{\text{box}} = \mathbf{B}_{dc} + \langle \mathbf{b} \rangle_{\text{box}}, \quad (8)$$

where $\langle \dots \rangle_{\text{box}}$ means a spatial average over the box. We then compute parallel and perpendicular (with respect to \mathbf{B}_0) structure functions, according to the definition given in Eq. (7) and with respect to \mathbf{B}_0 :

$$S_{\parallel}(l) \equiv S(\mathbf{I}_{\parallel}), \quad \text{where} \quad \mathbf{I}_{\parallel} \equiv l \frac{\mathbf{B}_0}{|\mathbf{B}_0|}, \quad (9)$$

$$S_{\perp}(l) \equiv S(\mathbf{I}_{\perp}), \quad \text{where} \quad \mathbf{I}_{\perp} \equiv l \frac{\hat{\mathbf{x}} \times \mathbf{B}_0}{|\hat{\mathbf{x}} \times \mathbf{B}_0|}. \quad (10)$$

The unit vector in the x direction [$\hat{\mathbf{x}}=(1,0,0)$] is arbitrarily chosen to obtain a direction which is perpendicular to \mathbf{B}_0 by means of the vector product. Note that in this scheme, both \mathbf{I}_{\parallel} and \mathbf{I}_{\perp} are functions of the position \mathbf{x} , since their orientation changes from box to box. Details on the implementation of Eqs. (9) and (10) are given in Appendix A.

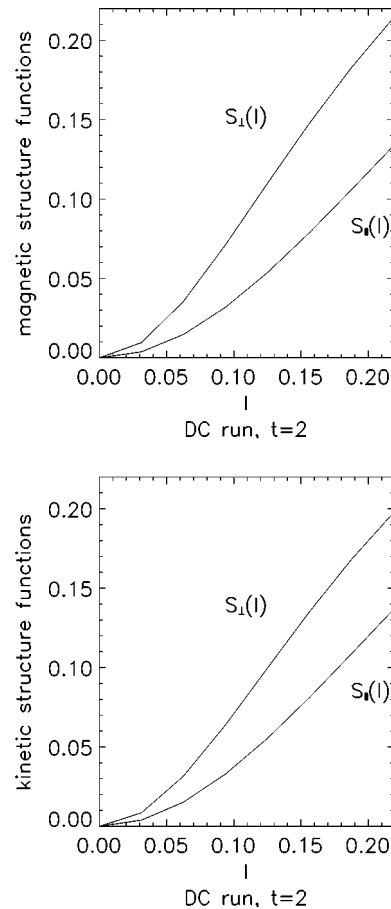


FIG. 2. Parallel and perpendicular structure functions for the dc run. The parallel direction is given by the dc field, $\mathbf{B}_{dc}=\hat{\mathbf{z}}$.

A comparison of Figs. 2 and 3 shows a slight increase in anisotropy when the local mean magnetic field is considered, instead of the global one. Thus, it seems natural that even when no dc field is present, the local mean field will give an anisotropy direction. This conjecture is confirmed in Sec. III C. Note that a quantitative measure of local anisotropy is needed to proceed. We address this issue in the next section.

B. Generalized anisotropy angles

In the presence of a dc magnetic field, a measure of the spectral anisotropy level is given by the *Shebalin angles*.² Let us choose a reference frame in which the dc field points in the $\hat{\mathbf{z}}$ direction. The Shebalin angle for the velocity field is given by

$$\tan^2(\theta) \equiv \frac{\sum_{\mathbf{k}} k_{\perp}^2 E_3^v(\mathbf{k})}{\sum_{\mathbf{k}} k_{\parallel}^2 E_3^v(\mathbf{k})}, \quad (11)$$

where $k_{\parallel}^2 = k_z^2$ and $k_{\perp}^2 = k_x^2 + k_y^2$. Note that the RHS in Eq. (11) gives an estimate of the ratio between a “typical” perpendicular wavenumber and a “typical” parallel wavenumber. Isotropy in the perpendicular planes (see, for instance, Fig. 1) allows us to rewrite Eq. (11) in terms of the reduced spectrum, either in the $\hat{\mathbf{x}}$ or in the $\hat{\mathbf{y}}$ direction:

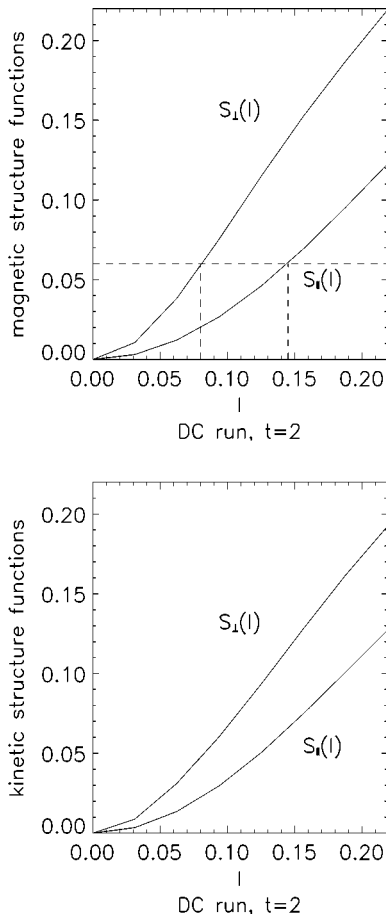


FIG. 3. Parallel and perpendicular structure functions for the dc run. The parallel direction is given by the local mean field, $\mathbf{B}_0 \equiv \mathbf{B}_{dc} + \langle \mathbf{b} \rangle_{\text{box}}$. The dashed lines illustrate a discussion from Sec. IV.

$$\tan^2(\theta) = 2\Gamma \equiv 2 \frac{\sum_k k_x^2 E_1^v(k_x)}{\sum_k k_z^2 E_1^v(k_z)}. \tag{12}$$

We can now write Γ in terms of structure functions, by noting that

$$\sum_{k_i} k_i^2 E_1^v(k_i) = \frac{1}{2} \langle |\partial_i \mathbf{v}|^2 \rangle = \lim_{l \rightarrow 0} \frac{S(l\hat{i})}{l^2}. \tag{13}$$

As a result,

$$\tan^2(\theta) = 2\Gamma = 2 \lim_{l \rightarrow 0} \frac{S(l\hat{x})}{S(l\hat{z})}. \tag{14}$$

If the field \mathbf{v} is isotropic, then $\Gamma=1$ and $\tan(\theta)=\sqrt{2}$.

Note that Eq. (14) involves the computation of structure functions which are either parallel or perpendicular with respect to the dc magnetic field direction. It seems natural to extend the definition to the general case in which the parallel and perpendicular directions are given either locally or globally (see the previous section):

$$\tan^2(\theta) = 2\Gamma \equiv 2 \lim_{l \rightarrow 0} \frac{S_{\perp}(l)}{S_{\parallel}(l)}. \tag{15}$$

By construction, definition (15) reduces to the classical definition (11) in the situation in which the parallel direction is given globally (by the direction of a dc magnetic field).

We can now give a quantitative measure of the increase in anisotropy observed in Fig. 3 with respect to Fig. 2, when considering the local mean field instead of the dc field. Estimating $\Gamma \approx S_{\perp}(\Delta l)/S_{\parallel}(\Delta l)$, where Δl is the grid size, we get the following:

- from Fig. 2, using the dc field: $\Gamma_b=2.5$; $\Gamma_v=2.2$;
- from Fig. 3, using the local mean field: $\Gamma_b=3.4$, $\Gamma_v=2.6$;

where Γ_b and Γ_v correspond, respectively, to structure functions computed for b and v . This confirms that anisotropy with respect to the local mean field is greater than anisotropy with respect to the dc field.

C. Local anisotropy with no dc field

We now analyze the results of the globally isotropic simulation, repeating the average procedure described in Sec. III A and Appendix A. Even though there is no dc magnetic field, the local mean magnetic field $\mathbf{B}_0 \equiv \langle \mathbf{B} \rangle_{\text{box}} = \langle \mathbf{b} \rangle_{\text{box}}$ provides a well defined direction with respect to which correlations are anisotropic, as we show below.

Motivated by definition (15) for the generalized anisotropy angles, we plot the ratio of perpendicular to parallel structure functions; Fig. 4 shows $S_{\perp}(l)/S_{\parallel}(l)$, for $t=0,1,2,3$. It is evident that anisotropy angles grow monotonically in time. This behavior indicates a dynamical build up of local anisotropy from the random isotropic initial condition. Note that the magnetic field is more anisotropic than the velocity field, a feature observed in numerical studies of global anisotropy.^{2,13}

Figure 5 shows the same ratio $S_{\perp}(l)/S_{\parallel}(l)$, at $t=3$, but computed following a conditional average procedure. The idea behind this procedure is to investigate the effect of the intensity of \mathbf{B}_0 . Only data coming from boxes in which the local mean field intensity B_0 is larger than a certain threshold is considered for the computation of both $S_{\perp}(l)$ and $S_{\parallel}(l)$ (see Appendix A for details). It is evident from the figure that such a conditional average gives stronger anisotropy for higher thresholds. That is: *anisotropy is bigger in regions of a strong magnetic field*. This result is consistent with previous results for the globally anisotropic case,^{5,6} in which spectral anisotropy is seen to increase linearly with the intensity of the dc applied field [specifically $\cos(\theta) \propto b/B_{dc}$, where b is the rms of the fluctuating magnetic field].

So far, the results for the analysis of anisotropy with respect to a locally defined \mathbf{B}_0 are intuitive, and provide a local version of the well known global anisotropy which arises in the presence of a dc magnetic field. It is also interesting to analyze the possible effect of a locally defined \mathbf{V}_0 . We address this in the next section.

D. The role of the local mean velocity field

There is a fundamental difference between the addition of a constant magnetic field and the addition of a constant velocity field to the MHD equations. While the latter has no

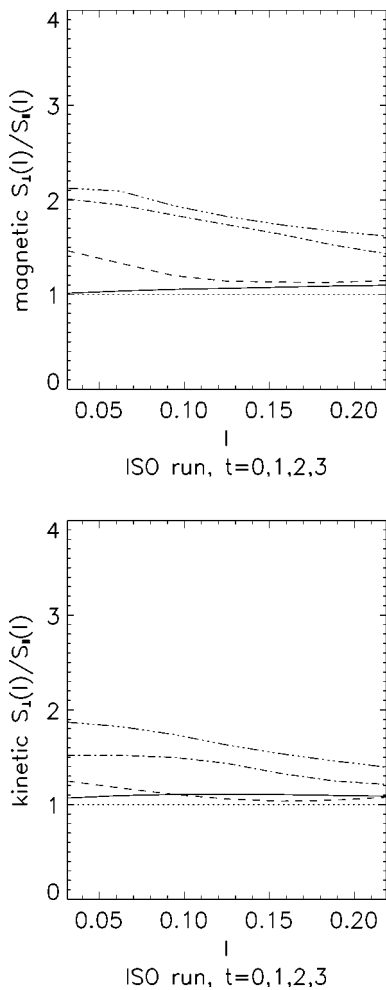


FIG. 4. The ratio between perpendicular and parallel structure functions for the ISO run, for different times: $t=0$ (continuous), $t=1$ (dashed), $t=2$ (dash-dot) and $t=3$ (dash-dot-dot-dot). The local mean \mathbf{B}_0 gives the parallel direction.

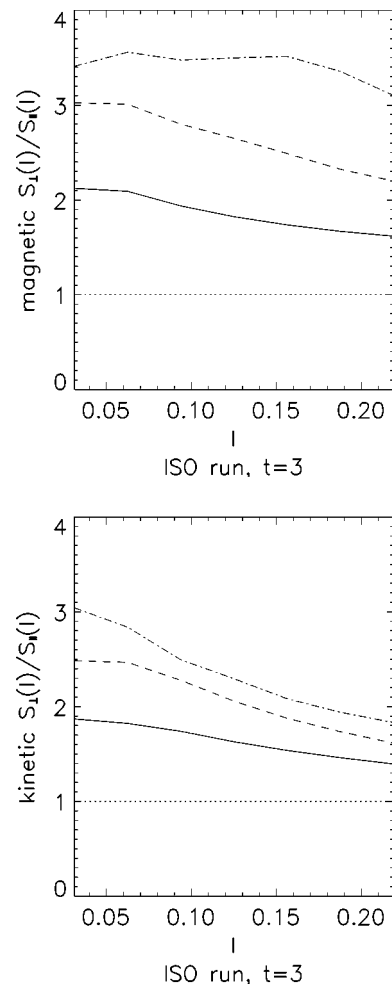


FIG. 5. The ratio between perpendicular and parallel structure functions for the ISO run. The local mean \mathbf{B}_0 gives the parallel direction. Threshold values are 0 (continuous), $\langle B_0 \rangle$ (dashed) and $\langle B_0 \rangle + \sigma$ (dashed-dotted), where $\langle B_0 \rangle$ and σ are, respectively, the mean and the standard deviation of B_0 over the values it takes at different boxes.

effect on the dynamics of the flow and can easily be removed through a Galilean transformation to a moving coordinate system, the former cannot be eliminated from the equations, and has the physical effect of propagation of perturbations in both directions along field lines, at the Alfvén speed.¹⁷ Therefore, we do not expect the local mean velocity field to produce local anisotropy. Notwithstanding, analysis of the role of \mathbf{V}_0 is to some extent subtle and certainly nontrivial, as follows.

To proceed, we define a local mean velocity field in the same spirit of Eq. (8),

$$\mathbf{V}_0 \equiv \langle \mathbf{v} \rangle_{\text{box}}, \tag{16}$$

and repeat the analysis of the previous section, following \mathbf{V}_0 (instead of \mathbf{B}_0) as the parallel direction. Figures 6 and 7 show the results thus obtained, which have to be contrasted to Figs. 4 and 5. It is clear that there is some level of anisotropy when the local \mathbf{V}_0 defines the local parallel direction. However, the amount of anisotropy is very low, giving rise to values of $\Gamma < 1.3$, which is fairly close to the isotropic value $\Gamma = 1$. It is also to be noted that, unlike what was observed in the previous section, anisotropy angles here neither

grow consistently in time (Fig. 6), nor do they as a function of the value of the threshold (Fig. 7). These results give a first indication that the role of \mathbf{V}_0 is not analogous to the role of \mathbf{B}_0 .

It has to be noticed that the directions given by \mathbf{V}_0 and \mathbf{B}_0 in our simulations are correlated, because of dynamical alignment,^{24,25} which tends to give finite $\langle |\mathbf{v} \cdot \mathbf{B}| \rangle$, even with zero cross helicity $\langle \mathbf{v} \cdot \mathbf{B} \rangle$.²⁶ Figure 8 illustrates this point, by displaying histograms of

$$\cos(\alpha) = \frac{\mathbf{v} \cdot \mathbf{B}}{|\mathbf{v}| |\mathbf{B}|}, \tag{17}$$

at different times. It is evident that the local alignment between \mathbf{v} and \mathbf{B} [which corresponds to $\cos(\alpha) \approx \pm 1$] tends to grow in time and is non-negligible, since then. As a consequence, \mathbf{V}_0 is somehow a surrogate for \mathbf{B}_0 , which is consistent with the small level of anisotropy observed in Figs. 6 and 7.

To test this interpretation, we study a purely hydrodynamic simulation. The results are shown in Figs. 9 and 10. In this case, $S_{\perp}(l)/S_{\parallel}(l)$ is even closer to the isotropic value of

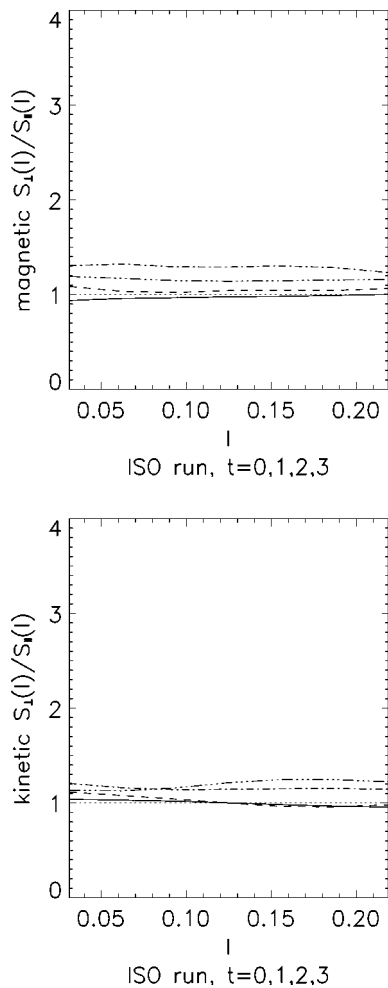


FIG. 6. The ratio between perpendicular and parallel structure functions for the ISO run, for different times: $t=0$ (continuous), $t=1$ (dashed), $t=2$ (dash-dot) and $t=3$ (dash-dot-dot-dot). The local mean \mathbf{V}_0 gives the parallel direction.

1, as compared to the MHD case (Figs. 6 and 7). We analyze this small level of anisotropy in Appendix B, where we show that the local analysis of anisotropy inherits some of the very well known kinematic anisotropy between lateral and longitudinal correlations in isotropic solenoidal vector fields.²⁷ Nonetheless, we stress that this is a small effect, and its contribution is negligible as compared to the levels of anisotropy induced dynamically by the local mean magnetic field.

IV. SUMMARY AND CONCLUSIONS

We present a study of local anisotropy in incompressible, 3D MHD. We seek for a local analog to the well established spectral anisotropy found in MHD turbulence, in the presence of a dc magnetic field.^{1,2} We perform 3D MHD pseudo-spectral incompressible relaxation simulations, and compute second order structure functions accumulated according to whether the separation is parallel to, or transverse to, the local magnetic field. The main result of the investigation can be phrased as follows: *the local mean magnetic field \mathbf{B}_0 produces local anisotropy for the correlations, even in cases in which the dynamical fields are globally isotropic* (i.e., when there is no magnetic dc field; see Sec. III C).

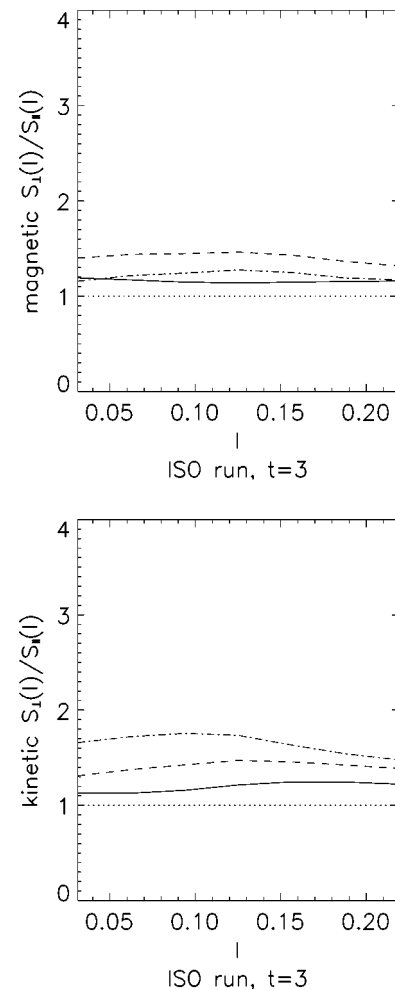


FIG. 7. The ratio between perpendicular and parallel structure functions for the ISO run. The local mean \mathbf{V}_0 gives the parallel direction. Threshold values are 0 (continuous), $\langle V_0 \rangle$ (dashed) and $\langle V_0 \rangle + \sigma$ (dash-dot), where σ is the standard deviation of V_0 over the values it takes at different boxes.

Correlation lengths are longer in the direction of the local mean magnetic field. We also find that in the presence of a dc magnetic field, local structure functions are more anisotropic if they are computed with respect to the local (instead

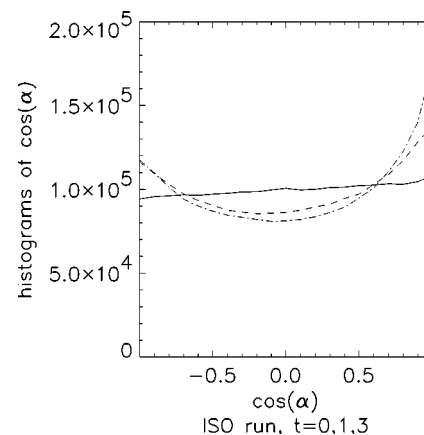


FIG. 8. Histograms of the cosine of the angle α between \mathbf{v} and \mathbf{B} for the ISO run, for different times: $t=0$ (continuous), $t=1$ (dashed) and $t=3$ (dash-dot). The histogram for $t=2$, which lies between the plots for $t=1$ and $t=3$, is omitted for clarity.

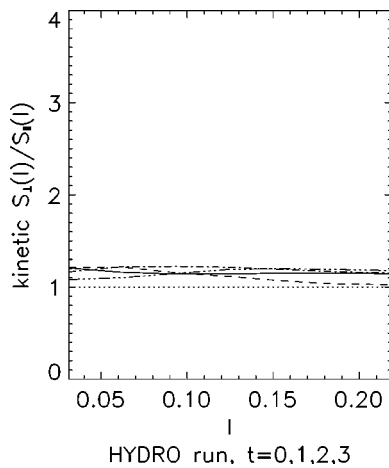


FIG. 9. The ratio between perpendicular and parallel structure functions for the HYDRO run. The local mean \mathbf{V}_0 gives the parallel direction. The intensity of the lines increases in time ($t=0,1,2,3$).

of the global) mean magnetic field (Sec. III A). Anisotropy is observed to be stronger in regions of a strong magnetic field (Fig. 5).

We propose in Sec. III B a generalization of the Shebalin anisotropy angles² which is suitable for the study of local anisotropy. Note that the RHS of Eq. (15) can be interpreted as the square of the ratio of the parallel Taylor microscale to the perpendicular Taylor microscale, which gives a simple interpretation to the definition. A paper on local anisotropy in globally anisotropic MHD turbulence (in the presence of a dc field) has been presented recently elsewhere.²⁸ In this work, local anisotropy is measured by means of second order structure functions, as well as we do here, but following a different method, which ultimately measures an anisotropic quantity which is not directly related to the Shebalin angles.²⁹ In contrast, our analysis is based on a generalization of the definition of global anisotropy angles which is

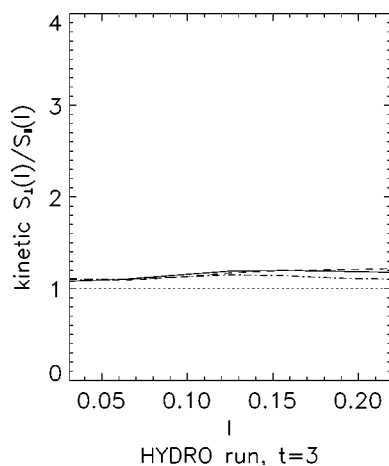


FIG. 10. The ratio between perpendicular and parallel structure functions for the HYDRO run. The local mean \mathbf{V}_0 gives the parallel direction. Threshold values are 0 (continuous), $\langle V_0 \rangle$ (dashed) and $\langle V_0 \rangle + \sigma$ (dash-dot), where σ is the standard deviation of V_0 over the values it takes at different boxes.

customary in the literature,^{2,5,6,13} as already mentioned, thus allowing a more straightforward link between the local and the global analysis of anisotropy.

We note in passing that, in showing that the appearance of spectral anisotropy is not dependent upon the simultaneous presence of a dc magnetic field and three-dimensional rectangular periodic boundary conditions, a potential conceptual objection to the latter³⁰ has been avoided; no magnetic field of a larger spatial scale than the dimension of the system being investigated is required. Instead, the correlation anisotropy is sustained entirely by local effects.

It could be questioned whether our results depend on the election of the size of the boxes used to average in order to obtain the local mean magnetic field. Our numerical exploration shows that the results do not depend qualitatively on the size of the boxes; furthermore, the quantitative dependence is weak, even though. Nonetheless, extremely high spatial resolution would be needed to explore box sizes sufficiently smaller than the energy containing scale (over which the average local magnetic field is meaningless as a direction in space) and big enough to avoid possible contamination from the solenoidal kinetic anisotropy discussed in Appendix B.

It is interesting to note that the magnetic field lines define locally two perpendicular directions: the normal and the binormal. Anisotropy in perpendicular planes, relative to these directions, may in principle occur (as it was suggested by a referee). However, note that our definition of a local mean field that is constant within each box, does not allow a computation of these directions (associated to the curvature of the field lines). On the other hand, the use of the local value of the magnetic field as a parallel direction would allow a study of this point, but would have some of the inconveniences described in Appendix B. A preliminary examination of this problem with our data seems to indicate that, if there exists anisotropy in perpendicular planes, it is much smaller than the anisotropy studied in this paper. A further analysis of this issue in a future work may lead to interesting results.

Other directions for future work are perhaps more straightforward. One would like to see how the local anisotropy depends on the Reynolds numbers, even though it is reasonable to expect a result consistent with the global one: that anisotropy increases with the value of the Reynolds numbers. It could also be interesting to study the scale dependence of anisotropy. Another interesting work would be to study the statistically steady turbulent regime by means of simulations with the addition of a forcing term. Finally, it would be interesting to see if compressible MHD turbulence develops local variance anisotropy, in analogy with the global case.²³

ACKNOWLEDGMENTS

This research was supported in part by the National Science Foundation under Grant No. ATM-9713595, and by the National Aeronautics and Space Administration Sun-Earth Connection Theory program at Bartol, NAG5-7164.

APPENDIX A: THE AVERAGE PROCEDURE

We discuss here some technical aspects on the computation of $S_{\parallel}(l)$ and $S_{\perp}(l)$ in terms of a local mean magnetic field. Since the calculation of these two quantities is totally analogous, we sometimes only mention $S_{\parallel}(l)$. As mentioned in Sec. III A, we divide the physical space in N_{box} boxes, and calculate a local mean magnetic field $\mathbf{B}_0 \equiv \langle \mathbf{B} \rangle_{\text{box}}$ in each box. We then compute, for each box, a local contribution to $S_{\perp}(l)$ and $S_{\parallel}(l)$, according to Eqs. (9) and (10). We finally average the contributions from all the boxes to get

$$S_{\parallel}(l) = \frac{1}{N_{\text{box}}} \sum_{i=1}^{N_{\text{box}}} S_{\parallel,i}(l), \quad (\text{A1})$$

where $S_{\parallel,i}(l)$ is the contribution from the i th box to the global result.

A procedure must still be prescribed to obtain $S_{\parallel,i}(l)$. Note that \mathbf{B}_0 is a discontinuous function of \mathbf{x} , the discontinuities lying in the boundaries between boxes. To avoid possible pathologies arising as a consequence of these discontinuities, we confine all computations within each box to a small region close to the center. We thus follow the following scheme:

- we fix one point, say \mathbf{x} , in the center of the box;
- we compute parallel and perpendicular displacements according to Eqs. (9) and (10), with $l = n\Delta l$, $n \in N$, $n < l_{\text{box}}/4\Delta l$, so that all separations are smaller than one fourth of the size of the boxes;
- we simply evaluate $S_{\parallel,i}(l) = \frac{1}{2} \langle |\mathbf{u}(\mathbf{x}) - \mathbf{u}(\mathbf{x} + \mathbf{l}_{\parallel})|^2 \rangle_{\text{box}}$.

Since $(\mathbf{x} + \mathbf{l}_{\parallel})$ is not necessarily a grid point, a linear interpolation method is used to evaluate $\mathbf{u}(\mathbf{x} + \mathbf{l}_{\parallel})$. The quantity $\frac{1}{2} \langle |\mathbf{u}(\mathbf{x}) - \mathbf{u}(\mathbf{x} + \mathbf{l}_{\parallel})|^2 \rangle$ has to be averaged over different values of \mathbf{x} . Due to the limitation in spatial resolution, we can only compute this average over a few values of \mathbf{x} for each box, and we do not find any significant impact of this local average in the results.

APPENDIX B: KINEMATIC VERSUS DYNAMIC ANISOTROPY

We analyze in this section an initial condition for \mathbf{B} . We recall that the initial conditions are homogeneous, isotropic and solenoidal, which implies that they obey the kind of anisotropy between longitudinal and lateral structure functions described by Batchelor.²⁷

We review here these results, adapted to our terminology and definitions. Consider longitudinal and lateral structure functions of the form

$$S_{\text{lon}}(l) \equiv \frac{1}{2} \langle |u_x(\mathbf{x}) - u_x(\mathbf{x} + l\hat{\mathbf{x}})|^2 \rangle, \quad (\text{B1})$$

$$S_{\text{lat}}(l) \equiv \frac{1}{2} \langle |u_x(\mathbf{x}) - u_x(\mathbf{x} + l\hat{\mathbf{y}})|^2 \rangle, \quad (\text{B2})$$

where $\hat{\mathbf{x}} \equiv (1, 0, 0)$ and $\hat{\mathbf{y}} \equiv (0, 1, 0)$ are orthogonal Cartesian unit vectors. Assuming the existence of an order-4 Taylor expansion for these quantities, and making use of the isotropy and homogeneity of the field \mathbf{u} , as well as the condition $\nabla \cdot \mathbf{u} = 0$, it is possible to show (see Ref. 27):

$$S_{\text{lon}}(l) = \frac{1}{2} \frac{u^2}{\lambda^2} l^2 + O(l^4), \quad (\text{B3})$$

$$S_{\text{lat}}(l) = \frac{u^2}{\lambda^2} l^2 + O(l^4), \quad (\text{B4})$$

where $u^2 \equiv u_x^2 = u_y^2 = u_z^2$ and $\lambda^2 = u^2/S''_{\text{lon}}(0)$. In analogy with Eq. (15), we define

$$\Gamma_{\text{Batchelor}} \equiv \lim_{l \rightarrow 0} \frac{S_{\text{lat}}(l)}{S_{\text{lon}}(l)} = 2, \quad (\text{B5})$$

where the last equality holds from Eqs. (B3) and (B4). This anisotropic behavior is purely kinematic. It does not depend on the structure of the dynamic equations for the field \mathbf{u} at all. It is to be stressed that definitions (15) and (B5) are not equivalent, since S_{\parallel} and S_{\perp} differ from S_{lon} and S_{lat} , as it is clear from the simple inspection of their definitions. Nonetheless, these quantities are related, as we show below.

Let us rewrite the magnetic structure functions, Eq. (7), as

$$S(\mathbf{l}) = \frac{1}{2} [\langle |\mathbf{B}(\mathbf{x})|^2 \rangle + \langle |\mathbf{B}(\mathbf{x} + \mathbf{l})|^2 \rangle - 2\langle \mathbf{B}(\mathbf{x}) \cdot \mathbf{B}(\mathbf{x} + \mathbf{l}) \rangle]. \quad (\text{B6})$$

The first term on the RHS of Eq. (B6) is just the total magnetic energy E^b . Due to homogeneity, if \mathbf{l} is a constant the second term on the RHS of Eq. (B6) is also equal to E^b . However, this result does not necessarily hold when \mathbf{l} is either parallel or perpendicular to the local mean magnetic field. Indeed, our simulations show that $\frac{1}{2} \langle |\mathbf{B}(\mathbf{x} + \mathbf{l})|^2 \rangle$ slightly departs from the constant value E^b as a function of l . The third term on the RHS of Eq. (B6) is the interesting one. Consider the case in which the point-wise local value of the field $\mathbf{B}(\mathbf{x})$, instead of the mean field \mathbf{B}_0 , is used to give the parallel and perpendicular directions in Eq. (B6). In this case, this term only involves longitudinal correlations when \mathbf{l}_{\parallel} is used [correlations of the component of \mathbf{B} which is parallel to the displacement \mathbf{l} , as in Eq. (B1)], and lateral correlations when \mathbf{l}_{\perp} is chosen. However, the angle between $\mathbf{B}(\mathbf{x})$ and \mathbf{l} takes any value without restrictions in definitions (B1) and (B2) for S_{lon} and S_{lat} , while this same angle is identically zero in definition (9) for S_{\parallel} and $\pi/2$ in definition (10) for S_{\perp} . In this regard, S_{\parallel} can be obtained from Eq. (B1), replacing the ensemble average operator by a conditional average operator, which only accepts data for the average when the angle between $\mathbf{B}(\mathbf{x})$ and \mathbf{l} is zero. Similarly, S_{\perp} could be obtained from definition (B1) for S_{lon} . However, we presently do not know of any analytical way of expressing the effect of such a replacement of the average operator. Moreover, when the local mean magnetic field \mathbf{B}_0 is used as the parallel direction, as we do in this paper, the relation between S_{\parallel} and S_{lon} , and between S_{\perp} and S_{lat} , is even more subtle. Therefore, we do not expect these quantities to be identical but we do not disregard a possible connection between them. To quantify this connection, we refer to our numerical results.

In Fig. 11 we plot the ratio of perpendicular to parallel magnetic structure functions for the initial condition of the ISO run, using in one case the local mean field \mathbf{B}_0 , and in the other case the local value $\mathbf{B}(\mathbf{x})$, as the parallel direction. Note that no dynamics are associated to the magnetic field at $t=0$, so that the only source of anisotropy could be the in-

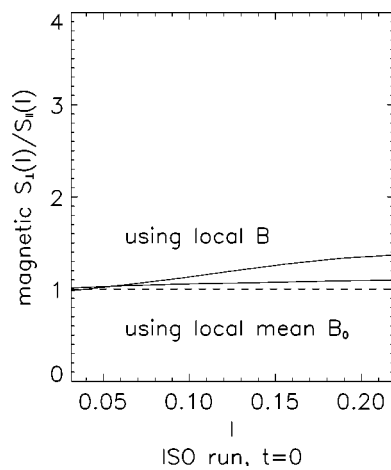


FIG. 11. The ratio between perpendicular and parallel structure functions for the initial condition of the ISO run. Upper line: The point-wise value $\mathbf{B}(\mathbf{x})$ gives the parallel direction. Lower line: The local mean \mathbf{B}_0 gives the parallel direction.

heritance of the kinematic anisotropy described above. The figure shows that this inheritance actually occurs, even though it is small: it gives an anisotropic contribution to S_{\perp}/S_{\parallel} of order ~ 0.1 , which has to be compared to dynamic anisotropies of order 1 measured in Figs. 1–5. It is interesting to note that, when we use the local average \mathbf{B}_0 instead of $\mathbf{B}(\mathbf{x})$, most of this effect is lost. We thus conclude that the local averaging process filters out part of the (undesired) inheritance of Batchelor's kinematic anisotropy.

- ¹D. Montgomery and L. Turner, Phys. Fluids **24**, 825 (1981).
²J. V. Shebalin, W. H. Matthaeus, and D. Montgomery, J. Plasma Phys. **29**, 525 (1983).
³C. S. Ng and A. Bhattacharjee, Astrophys. J. **465**, 845 (1996).
⁴R. M. Kinney and J. C. McWilliams, Phys. Rev. E **57**, 7111 (1998).
⁵W. H. Matthaeus, S. Oughton, S. Ghosh, and M. Hossain, Phys. Rev. Lett. **81**, 2056 (1998).
⁶S. Oughton, W. H. Matthaeus, and S. Ghosh, Phys. Plasmas **5**, 4235 (1998).
⁷K. Nakayama, Astrophys. J. **523**, 315 (1999).

- ⁸D. C. Robinson, M. G. Rusbridge, and P. A. Saunter, Plasma Phys. **10**, 1005 (1968).
⁹M. G. Rusbridge, Plasma Phys. **11**, 35 (1969).
¹⁰D. C. Robinson and M. G. Rusbridge, Phys. Fluids **14**, 2499 (1971).
¹¹W. H. Matthaeus, M. L. Goldstein, and D. A. Roberts, J. Geophys. Res. **95**, 20 673 (1990).
¹²J. Armstrong, W. Coles, M. Kojima, and B. Rickett, Astrophys. J. **358**, 685 (1990).
¹³S. Oughton, E. R. Priest, and W. H. Matthaeus, J. Fluid Mech. **280**, 95 (1994).
¹⁴S. Sridhar and P. Goldreich, Astrophys. J. **432**, 612 (1994).
¹⁵D. Montgomery and W. H. Matthaeus, Astrophys. J. **447**, 706 (1995).
¹⁶S. Galtier, S. V. Nazarenko, A. C. Newell, and A. Pouquet, J. Plasma Phys. **63**, 447 (2000).
¹⁷W. M. Elsässer, Phys. Rev. **79**, 183 (1950).
¹⁸B. B. Kadomtsev and O. P. Pogutse, Sov. Phys. JETP **38**, 283 (1974).
¹⁹H. R. Strauss, Phys. Fluids **19**, 134 (1976).
²⁰D. Montgomery, Phys. Scr. **T2/1**, 83 (1982).
²¹G. P. Zank and W. H. Matthaeus, J. Plasma Phys. **48**, 85 (1992).
²²P. Goldreich and S. Sridhar, Astrophys. J. **438**, 763 (1995).
²³W. H. Matthaeus, S. Ghosh, S. Oughton, and D. A. Roberts, J. Geophys. Res. **101**, 7619 (1996).
²⁴M. Dobrowolny, A. Mangeney, and P. Veltri, Phys. Rev. Lett. **45**, 144 (1980).
²⁵A. Pouquet, U. Frisch, and M. Meneguzzi, Phys. Rev. A **33**, 4266 (1986).
²⁶A. C. Ting, D. Montgomery, and W. H. Matthaeus, Phys. Fluids **29**, 3261 (1986).
²⁷G. K. Batchelor, in *The Theory of Homogeneous Turbulence*, edited by G. K. Batchelor and H. Bondi (Cambridge University Press, Cambridge, 1953), Chap. 3.
²⁸J. Cho and E. T. Vishniac, Astrophys. J. **539**, 273 (2000).
²⁹As implied by Eq. (15), it is the ratio of perpendicular to parallel structure functions that measures anisotropy in the usual way. However, in Ref. 28 Shebalin angles are estimated [see Eq. (14) in Ref. 28] by looking at contours of a constant value for second order correlation functions in a plane $(l_{\parallel}, l_{\perp})$ (Fig. 8 in Ref. 28). From the intercepts of these contours with each axis they extract a parallel and a perpendicular length and they consider the ratio of this length as a measure of the anisotropy at this spatial scale. The translation of this procedure to our work is sketched in Fig. 3, in dashed lines. The two vertical dashed lines correspond to values of l for which the structure functions are the same, i.e., $S_{\parallel}(l=0.08) = S_{\perp}(l=0.145) = 0.06$. Thus, $l_{\perp}/l_{\parallel} = 0.145/0.08 \approx 1.8$ would give a measure of the anisotropy at a scale $l \sim 0.1$. We stress that, according to definition (15) for the generalized Shebalin angles, the anisotropy (either global or local) is measured by $\Gamma = \lim_{l \rightarrow 0} S_{\perp}(l)/S_{\parallel}(l)$ ($= 3.4$ in Fig. 3—top), which is a totally different quantity.
³⁰D. C. Montgomery and J. W. Bates, Phys. Plasmas **6**, 2727 (1999).